CFD VALIDATION STUDY:

S60 - CALM WATER

NepTech

Intelligent sea mobility

Version	Date	Written by	Validated by
1	XX/XX/XXXX	Tanguy TEULET	Clément ROUSSET

Table of contents

Summary

This report provides a comprehensive validation study on the Series 60 catamaran in calm water, using NepTech's digital towing tank. The study covers a range of Froude numbers from 0.15 to 0.55 and includes various hull spacings to reflect different catamaran configurations. Key findings compare CFD results with experimental data, addressing resistance, vessel motions, free surface renderings, and computational time. The results confirm that NepTech's automated digital towing tank is reliable and efficient for simulating multihull vessels at both low and medium Froude numbers, validating its capabilities for accurate predictions in similar flow types.

Nomenclature

- $\frac{B_{WL}}{T}$ $[-]$, beam-draft ratio.
- $\frac{L_{WL}}{B_{WL}}$ $[-]$, length-beam ratio.
- B_{WL} $[m]$, waterline beam.
- C_B $[-]$, block coefficient.
- F_n $[-]$, Froude number.
- L_{PP} $[m]$, length between perpendiculars.
- $S_w[m^2]$, wetted surface.
- Δ $[kg]$, displacement.
- CFD, Computational Fluid Dynamic.
- EFD, Experimental Fluid Dynamic.
- LCG ; TCG ; VCG $[m]$, coordinates of the centre of gravity: lateral, transversal and vertical.
- s $[m]$, Distance between the demi hull centres.
- T $[m]$, draft.
- V $[m/s]$, ship speed.
- μ $[Pa.s]$, dynamic viscosity.
- ρ $[kg/m^3]$, density.

Figures

Tables

1. Series 60

This study aims to validate the accuracy of Computational Fluid Dynamics (CFD) simulations by comparing them with experimental data obtained by the *Model Basin Research Group (CEHINAV)* in June 2012. The reference paper, *"Experimental Assessment of Interference Resistance for a Series 60 Catamaran in Free and Fixed Trim-Sinkage Conditions"*, conducted by Antonio Souto-Iglesias, David Fernandez-Gutierrez, and Luis Perez-Rojas, provides a well-established dataset for evaluating hydrodynamic performance in multihull configurations.

The objective is to assess the reliability of NepTech's digital test basin by reproducing the experimental conditions and comparing the results in terms of hydrodynamic resistance, trim, and sinkage. The study considers both the monohull case and the catamaran configuration, with different float spacings: 565 mm, 768 mm, 971 mm, and 1174 mm. It is important to note that the analysis of the influence of float spacing on hydrodynamic performance will be addressed in a dedicated report. Here, the focus is solely on comparing numerical results with experimental data using the dataset provided in the reference study.

The selected hull model is based on the Series 60, a well-documented hull form widely used for hydrodynamic research due to its systematic geometric characteristics and applicability in performance assessments. Two main configurations are considered:

- Monohull case, serving as a reference to evaluate the resistance of a single hull and to provide a baseline for interference analysis in multihull configurations.
- Catamaran case, where the distance between the floats is gradually increased (565 mm, 768 mm, 971 mm, and 1174 mm) to analyse the impact of hull spacing on total resistance and hydrodynamic interactions.

These simulations will help quantify discrepancies between experimental and numerical results, providing a robust validation framework for NepTech's digital test basin.

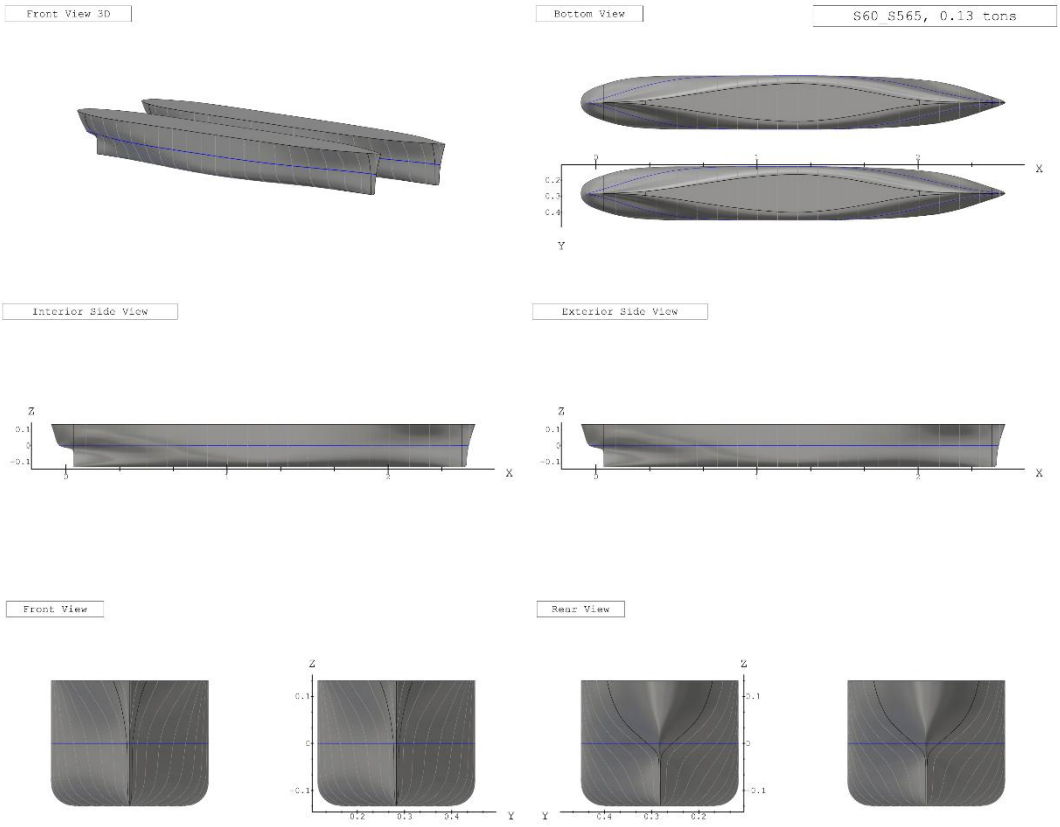

Figure 1: S60_S565 CAD model

2. Simulation setup

a. Sign convention

Heave: The heave values correspond to the dynamic elevation of the vessel at the centre of gravity, relative to its hydrostatic position, in the absolute reference frame with the vertical axis Z oriented upwards. A positive heave value thus corresponds to a hull rise, while a negative value indicates the hull sinking.

Pitch: The pitch values correspond to the dynamic trim of the vessel at the centre of gravity, relative to its hydrostatic position, in the absolute reference frame where the transverse axis is Y. A positive trim corresponds to a bow-up attitude of the hull.

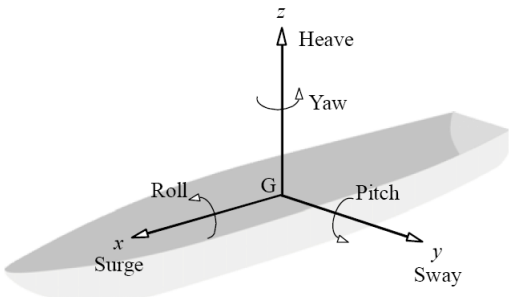

Figure 2: Sign convention illustration

b. Software's

Mesh: Hexpress™, version 12.1 developed by CADENCE

Resolution: Fidelity Fine Marine, version 12.1 developed by CADENCE

Solver: ISIS-CFD developed by CNRS and Centrale Nantes

Computing infrastructure: 2 virtual machines with 32 cores « C2D_STANDARD_32 », optimized for computation on Google Cloud Platform.

Post-processing:

- CFView™, version 12.1 developed by CADENCE
- Programming language Python version 3.11.6

c. Hypothesis

Modelling scale: model scale, with a symmetry plane along the vessel's median axis. This approach helps reduce computation time while maintaining identical results.

Domain: the dimensions of the simulation domain are conformed to International Towing Tank Conference (ITTC) recommendations, ensuring that the boundaries are positioned sufficiently far from the vessel to avoid any influence on the solution. It is crucial, especially for the exit boundary, to place it in a way that prevents the reflection of the wave field generated by the vessel.

Hydrostatic equilibrium: the coordinates of the centre of gravity are defined as follows

$$LCG = 1.212\,m;\ TCG = 0.000\,m;\ VCG = 0.021\,m$$

Water: corresponds to fresh water, which is

$$\rho_{water} = 997.561\ kg/m^3$$

$$\mu_{water} = 0.932 * 10^{-3}\ Pa.s$$

Air: corresponds to air at a temperature of $15°C$, which is

$$\rho_{air} = 1.2256\ kg/m^3$$

$$\mu_{air} = 1.788 * 10^{-5}\ Pa.s$$

Mesh precision: this report presents the results from medium level meshes.

d. Numerical models

Dynamic equilibrium:

- The Quasi-Static (QS) method is used since we are interested in the vessel's dynamic equilibrium state. This method relies on a succession of predictions of the vessel's physical attitude to reach the dynamic equilibrium state in record time.
- Two movements of the vessel, heave and pitch, are left free to ensure convergence toward the vessel's dynamic equilibrium position.

Flow: The Reynolds-Averaged Navier-Stokes (URANS) equations are used to describe the flow, and they are coupled with the $k - \omega\ SST$ turbulence model as the closure model.

Free surface: The air-water interface is modelled using the Volume of Fluid (VoF) method. Adaptive Grid Refinement (AGR), developed by CNRS (French National Centre for Scientific Research) and Ecole Centrale de Nantes (French Engineering school), is used to model the free surface. This iterative process allows for dynamic adjustment of the mesh according to the solution's needs during the calculation, making refinement decisions based on the physics of the flow.

e. Validation

i. Mesh

Free surface: The accuracy of the results regarding pressure resistance mainly depends on how the air-water interface is captured during simulation. This resistance is induced by the wave field generated by the vessel, and the quality of the mesh for the latter plays a crucial role in this accuracy. The use of AGR allows dynamically adapting the mesh based on the generated wave field, achieving maximum precision, as it is one of the most advanced and reliable methods to date and reducing computation time by converging more quickly toward the dynamic equilibrium state.

Hull: The accuracy of the results regarding viscous resistance mainly depends on the mesh of the hull. This resistance is caused by the entrainment of a thin fluid film: the boundary layer. An appropriate mesh of the boundary layer is essential to correctly capture local phenomena such as viscous effects and rapid variations in fluid properties near the surface. It also allows for better capture and resolution of turbulent phenomena if they are present. The quality of the hull mesh also affects the fidelity of the 3D model representation. A clean and regular mesh improves the reliability of the simulation, making the simulated model more representative of the actual vessel.

Ship speed $\mathbf{V}$	$[\mathbf{m/s}]$	0.74	0.99	1.24	1.49	1.73	1.98	2.23	2.48	2.72
	$[\mathbf{knots}]$	1.44	1.93	2.41	2.89	3.37	3.85	4.33	4.81	5.30
Froude number $\mathbf{F_n}$ $[-]$		0.15	0.20	0.25	0.30	0.35	0.40	0.45	0.50	0.55
Averaged number of cells [*10^6]	S60_Mono	0.95	0.95	0.96	1.02	1.03	1.09	1.22	1.29	1.33
	S60_S565	1.81	1.83	1.84	1.97	2.02	2.15	2.96	2.80	2.57
	S60_S768	1.82	1.84	1.85	1.99	2.02	2.12	2.86	2.57	2.57
	S60_S971	1.84	1.86	1.86	1.98	2.03	2.16	2.53	2.52	2.54
	S60_S1174	1.84	1.85	1.87	1.99	2.03	2.13	2.45	2.56	2.61

Table 1: Averaged number of cells

ii. Courant number

Description: The Courant number, also called the CFL (Courant-Friedrichs-Lewy) number, is a crucial parameter in computational fluid dynamics (CFD). It measures the numerical stability of the discretization scheme used in the simulation. An inappropriate Courant number can lead to numerical instabilities, compromising both convergence and the accuracy of the results. In CFD, the Courant number is related to the size of the numerical time steps. It is calculated by comparing the speed of fluid particles with the size of the cells in the simulation domain.

Recommended values: For typical resistance simulations, it is recommended to keep the Courant number below or close to 1 to ensure maximum accuracy and reliability. Local spikes in this parameter may occur, but it is essential to control them to maintain numerical stability and the quality of the results.

Values:

Ship speed $\mathbf{V}$	$[\mathbf{m/s}]$	0.74	0.99	1.24	1.49	1.73	1.98	2.23	2.48	2.72
	$[\mathbf{knots}]$	1.44	1.93	2.41	2.89	3.37	3.85	4.33	4.81	5.30
Froude number $\mathbf{F_n}$ $[-]$		0.15	0.20	0.25	0.30	0.35	0.40	0.45	0.50	0.55
Averaged Courant number [-]	S60_Mono	0.07	0.08	0.08	0.10	0.10	0.13	0.17	0.20	0.22
	S60_S565	0.09	0.10	0.10	0.13	0.14	0.18	0.30	0.38	0.37
	S60_S768	0.09	0.11	0.11	0.14	0.14	0.21	0.32	0.34	0.34
	S60_S971	0.10	0.11	0.11	0.13	0.15	0.22	0.28	0.32	0.32
	S60_S1174	0.10	0.11	0.11	0.14	0.15	0.21	0.27	0.31	0.32

Table 2: Averaged Courant number (Free Surface)

Ship speed V	$[m/s]$	0.74	0.99	1.24	1.49	1.73	1.98	2.23	2.48	2.72
	$[knots]$	1.44	1.93	2.41	2.89	3.37	3.85	4.33	4.81	5.30
Froude number F_n $[-]$		0.15	0.20	0.25	0.30	0.35	0.40	0.45	0.50	0.55
Averaged Courant number [-]	S60_Mono	1.46	1.51	1.55	1.45	1.48	1.54	1.59	1.59	1.58
	S60_S565	1.49	1.53	1.57	1.51	1.55	1.58	1.75	1.70	1.63
	S60_S768	1.45	1.50	1.53	1.47	1.52	1.63	1.66	1.58	1.58
	S60_S971	1.47	1.51	1.55	1.46	1.50	1.60	1.60	1.57	1.54
	S60_S1174	1.47	1.51	1.55	1.45	1.49	1.57	1.59	1.57	1.55

Table 3: Averaged Courant number (Hull)

iii. Y+

Description: In the naval field, managing the Y+ parameter is crucial in computational fluid dynamics (CFD) simulations. Y+ measures the quality of the boundary layer resolution along the submerged surfaces of ship hulls by evaluating the distance between the first mesh point and the wall relative to the boundary layer thickness. Maintaining an appropriate Y+ is essential to ensure reliable results in predicting resistance, drag, lift, and other critical hydrodynamic phenomena. An improper Y+ can lead to significant errors in the prediction of forces, drag coefficients, and other key parameters.

Recommended values: For typical resistance simulations, it is recommended that the Y+ value be between 30 and 300. This value may be lower depending on the choice of boundary layer modeling. Local spikes in this parameter may occur, but it is essential to control them to maintain numerical stability and the quality of the results.

Values:

Ship speed V	$[m/s]$	0.74	0.99	1.24	1.49	1.73	1.98	2.23	2.48	2.72
	$[knots]$	1.44	1.93	2.41	2.89	3.37	3.85	4.33	4.81	5.30
Froude number F_n $[-]$		0.15	0.20	0.25	0.30	0.35	0.40	0.45	0.50	0.55
Averaged Y+ [-]	S60_Mono	44.26	57.58	70.54	42.56	48.92	55.87	62.97	69.48	75.59
	S60_S565	45.00	58.43	71.66	43.38	49.57	55.11	64.06	71.42	76.90
	S60_S768	44.51	57.85	70.76	43.15	49.56	56.75	64.62	70.44	76.03
	S60_S971	44.75	58.21	71.25	43.11	49.27	56.85	64.10	70.15	75.88
	S60_S1174	44.69	58.13	71.17	42.97	49.30	56.84	63.88	70.01	75.94

Table 4: Averaged Y+

3. Geometry and hydrostatic

The numerical model used for the CFD simulations demonstrates a very strong alignment with the experimental model used in the towing tank tests in terms of hydrostatic characteristics, which is crucial for ensuring the validity of the comparison between numerical and experimental results. Hydrostatic parameters such as displacement, draft, and hull shape significantly influence the flow behaviour around the hull, directly affecting the prediction of resistance and hydrodynamic performance.

Table 5 summarizes these differences.

The strong agreement in hydrostatic characteristics reinforces confidence in the numerical model's accuracy, ensuring that the comparison with the physical model remains meaningful and reliable.

Main particulars		EFD	CFD	Difference [%]
Length between perpendiculars	L_{PP} $[m]$	2.500	2.505	+0.20
Beam at waterline	B_{WL} $[m]$	0.333	0.333	0.00
Draft	T $[m]$	0.133	0.132	-0.75
Wetted surface	$S_w[m^2]$	1.062	1.064	+0.19
Displacement	Δ $[kg]$	65.70	65.70	0.00
Block coefficient	C_B $[-]$	0.600	0.588	-2.00
Length-beam ratio	$\frac{L_{WL}}{B_{WL}}$ $[-]$	7.51	7.63	+1.60
Beam-draft ratio	$\frac{B_{WL}}{T}$ $[-]$	2.50	2.52	+0.80

Table 5: Geometry and hydrostatic

4. Results

a. Resistance

The drag resistance of the Series 60 monohull and catamaran at the different float spacings across different advance speeds are illustrates in the top graph and table of:

- Figure 3: S60_Mono evolution, difference in [%] and [N] of drag resistance
- Figure 4: S60_S565 evolution, difference in [%] and [N] of drag resistance
- Figure 5: S60_S768 evolution, difference in [%] and [N] of drag resistance
- Figure 6: S60_S971 evolution, difference in [%] and [N] of drag resistance
- Figure 7: S60_S1174 evolution, difference in [%] and [N] of drag resistance

The middle table displays the relative difference between CFD and EFD as a percentage, while the bottom table shows the absolute differences between CFD and EFD in international units:

$$E\%\ CFD = \frac{CFD - EFD}{EFD} * 100$$

To thoroughly assess results, particularly percentage differences, it is important to consider both percentage and absolute values. In comparisons with towing tank tests, target resistance values are very low, so even minor discrepancies can lead to large percentage errors.

The resistance error ranges from:

- **-5.25 to +3.54 percents and from -0.21 to +1.13 Newtons for the S60_Mono hull.**
- **-4.92 to +1.08 percents and from -1.18 to +0.05 Newtons for the S60_S565 hull.**
- **-2.53 to +7.88 percents and from -2.63 to +1.38 Newtons for the S60_S768 hull.**
- **-5.65 to +6.64 percents and from -3.42 to +1.74 Newtons for the S60_S971 hull.**
- **-3.48 to +4.08 percents and from -2.90 to +1.25 Newtons for the S60_S1174 hull.**

The resistance error between the EFD and CFD simulations is on the order of Newtons, demonstrating excellent agreement at most speeds, particularly due to the very similar trends observed in the curves.

The analysis of the results highlights that the largest discrepancies occur at a Froude number of 0.40 for the monohull case S60_Mono and at 0.45 for the catamaran cases S60_S565, S60_S768, and S60_S971. For the S60_S1174 catamaran, the most critical range is between Froude 0.35 and 0.50. This clearly illustrates the challenge of accurately resolving transitional speeds numerically, particularly within the Froude 0.4 to 0.6 range, where the dynamic of the vessels is more complex.

Furthermore, in catamaran configurations, wave interactions introduce additional complexity, leading to larger errors compared to the monohull case. Specifically, at Froude 0.45, the numerical model tends to underestimate the additional resistance due to float spacing. This discrepancy may also be attributed to differences in hydrostatic characteristics:

- The numerical model has a slightly greater waterline length than the experimental model, which could result in weaker wave interactions and therefore lower resistance predictions.
- Additionally, the block coefficient of the numerical model is lower, potentially leading to a reduced wave resistance, especially when the additional resistance due to float spacing become significant.

This hypothesis are further supported by the fact that at higher speeds, where the Kelvin wave angle becomes very narrow and wave interactions diminish, the CFD and experimental resistance curves converge more closely.

Significant deviations are also observed around Froude numbers of 0.20 to 0.25 for all configurations. This behaviour is entirely expected at low speeds, as the total resistance is only a few Newtons in this range, and the wake generated by the vessel is weak in amplitude. As a result, capturing the wake with high precision becomes particularly challenging, making the resistance prediction highly sensitive to small variations.

i. S60_Mono

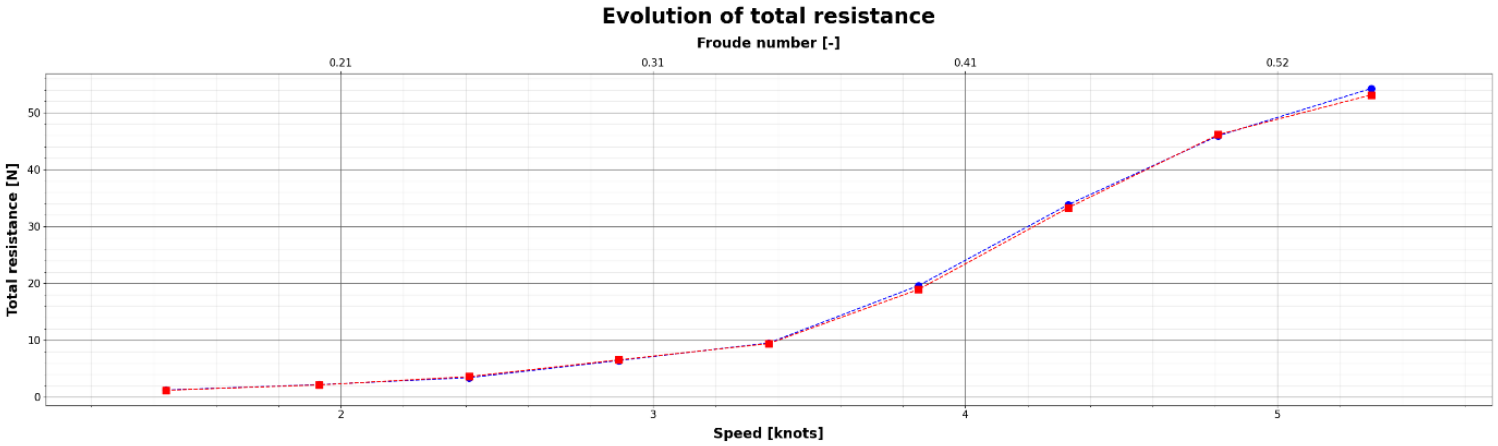

	Speed [knots]	Froude number [-]	● Total resistance [N], S60_Mono	■ Total resistance [N], S60_Mono_EFD
0	1.44	0.15	1.26	1.22
1	1.93	0.20	2.21	2.16
2	2.41	0.25	3.43	3.62
3	2.89	0.30	6.44	6.56
4	3.37	0.35	9.53	9.42
5	3.85	0.40	19.60	18.93
6	4.33	0.45	33.84	33.30
7	4.81	0.50	45.93	46.14
8	5.30	0.55	54.24	53.11

	Speed [knots]	Froude number [-]	X_0 = S60_Mono, [%]
0	1.44	0.15	3.28
1	1.93	0.20	2.31
2	2.41	0.25	-5.25
3	2.89	0.30	-1.83
4	3.37	0.35	1.17
5	3.85	0.40	3.54
6	4.33	0.45	1.62
7	4.81	0.50	-0.46
8	5.30	0.55	2.13

	Speed [knots]	Froude number [-]	X_0 = S60_Mono, [N]
0	1.44	0.15	0.04
1	1.93	0.20	0.05
2	2.41	0.25	-0.19
3	2.89	0.30	-0.12
4	3.37	0.35	0.11
5	3.85	0.40	0.67
6	4.33	0.45	0.54
7	4.81	0.50	-0.21
8	5.30	0.55	1.13

Figure 3: S60_Mono evolution, difference in [%] and [N] of drag resistance

ii. S60_S565

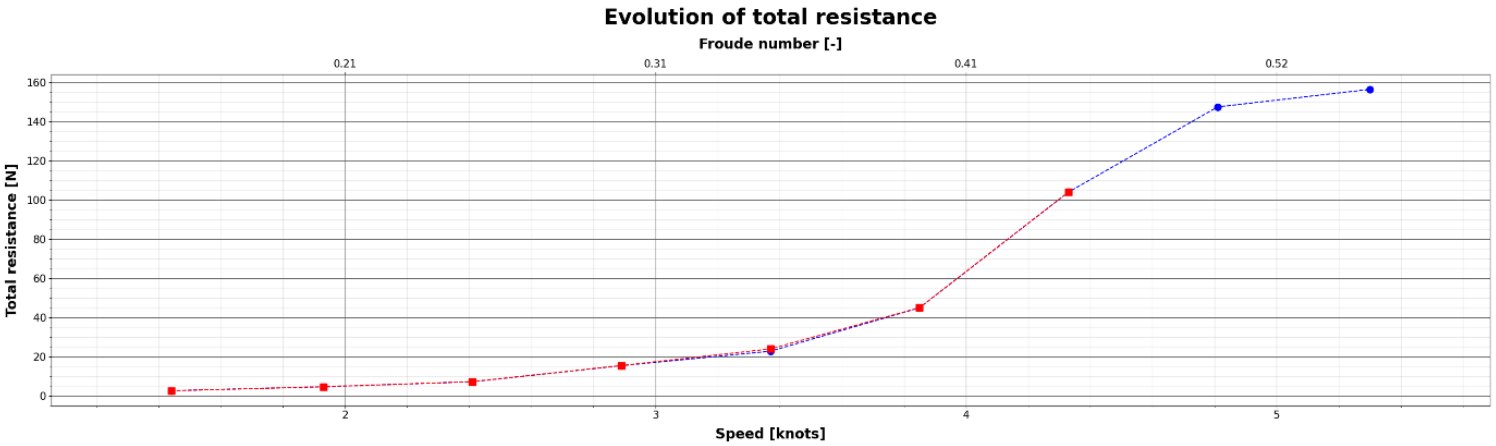

	Speed [knots]	Froude number [-]	● Total resistance [N], S60_S565	■ Total resistance [N], S60_S565_EFD
0	1.44	0.15	2.64	2.65
1	1.93	0.20	4.66	4.61
2	2.41	0.25	7.20	7.29
3	2.89	0.30	15.42	15.49
4	3.37	0.35	22.80	23.98
5	3.85	0.40	44.94	45.01
6	4.33	0.45	104.00	104.07
7	4.81	0.50	147.43	X
8	5.30	0.55	156.38	X

	Speed [knots]	Froude number [-]	X_0 = S60_S565, [%]
0	1.44	0.15	-0.38
1	1.93	0.20	1.08
2	2.41	0.25	-1.23
3	2.89	0.30	-0.45
4	3.37	0.35	-4.92
5	3.85	0.40	-0.16
6	4.33	0.45	-0.07

	Speed [knots]	Froude number [-]	X_0 = S60_S565, [N]
0	1.44	0.15	-0.01
1	1.93	0.20	0.05
2	2.41	0.25	-0.09
3	2.89	0.30	-0.07
4	3.37	0.35	-1.18
5	3.85	0.40	-0.07
6	4.33	0.45	-0.07

Figure 4: S60_S565 evolution, difference in [%] and [N] of drag resistance

iii. S60_S768

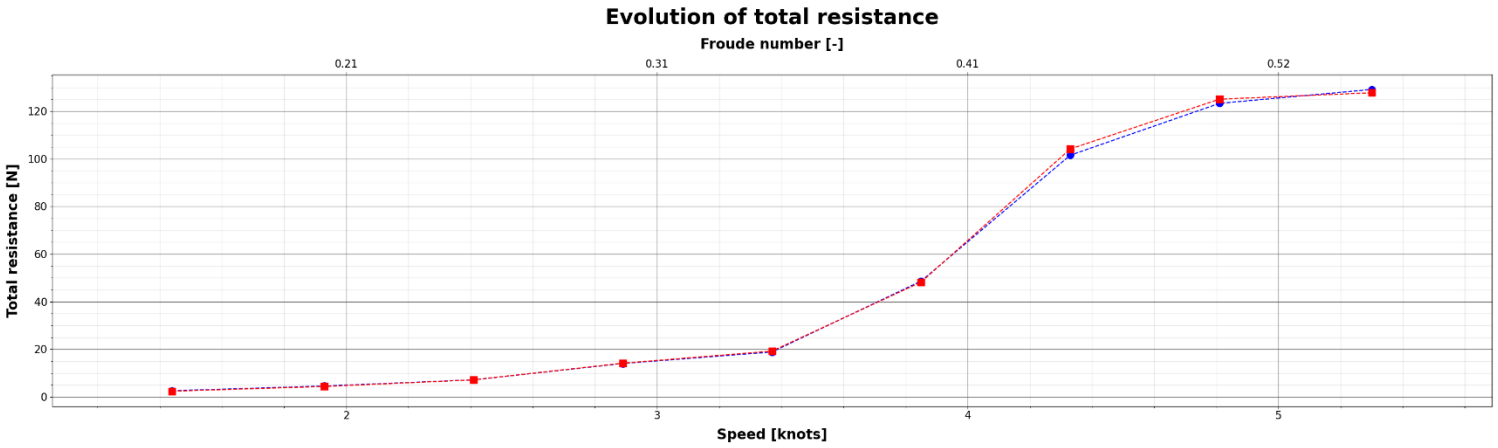

	Speed [knots]	Froude number [-]	● Total resistance [N], S60_S768	■ Total resistance [N], S60_S768_EFD
0	1.44	0.15	2.60	2.41
1	1.93	0.20	4.57	4.38
2	2.41	0.25	7.17	7.17
3	2.89	0.30	14.03	14.15
4	3.37	0.35	18.86	19.24
5	3.85	0.40	48.65	48.22
6	4.33	0.45	101.50	104.13
7	4.81	0.50	123.27	125.02
8	5.30	0.55	129.10	127.72

	Speed [knots]	Froude number [-]	X_0 = S60_S768, [%]
0	1.44	0.15	7.88
1	1.93	0.20	4.34
2	2.41	0.25	0.00
3	2.89	0.30	-0.85
4	3.37	0.35	-1.98
5	3.85	0.40	0.89
6	4.33	0.45	-2.53
7	4.81	0.50	-1.40
8	5.30	0.55	1.08

	Speed [knots]	Froude number [-]	X_0 = S60_S768, [N]
0	1.44	0.15	0.19
1	1.93	0.20	0.19
2	2.41	0.25	0.00
3	2.89	0.30	-0.12
4	3.37	0.35	-0.38
5	3.85	0.40	0.43
6	4.33	0.45	-2.63
7	4.81	0.50	-1.75
8	5.30	0.55	1.38

Figure 5: S60_S768 evolution, difference in [%] and [N] of drag resistance

iv. S60_S971

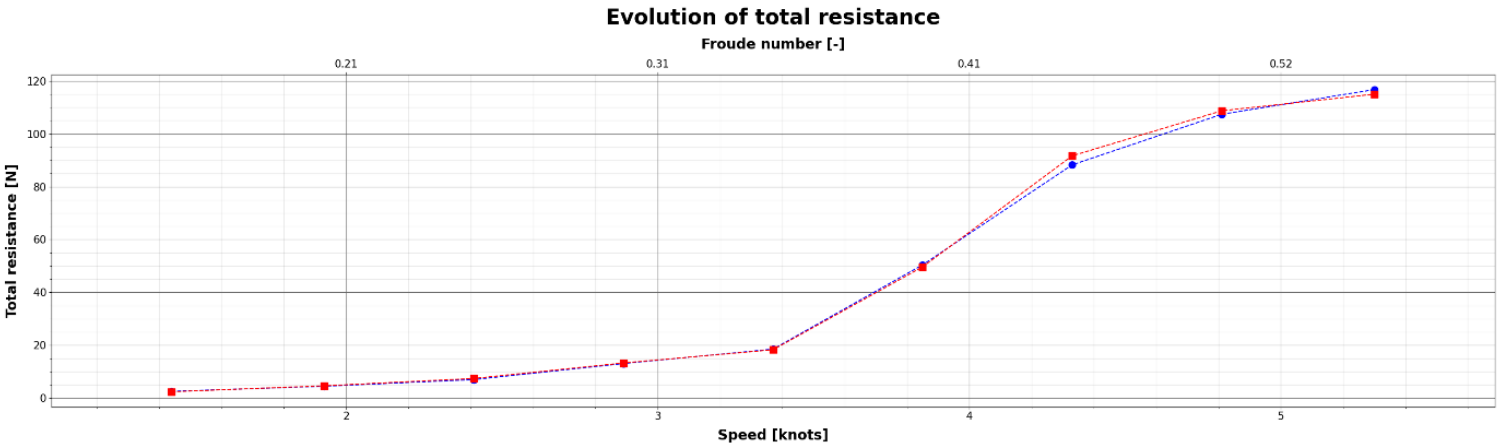

	Speed [knots]	Froude number [-]	● Total resistance [N], S60_S971	■ Total resistance [N], S60_S971_EFD
0	1.44	0.15	2.57	2.41
1	1.93	0.20	4.49	4.66
2	2.41	0.25	7.01	7.43
3	2.89	0.30	13.08	13.30
4	3.37	0.35	18.53	18.30
5	3.85	0.40	50.42	49.66
6	4.33	0.45	88.25	91.67
7	4.81	0.50	107.39	108.72
8	5.30	0.55	116.73	114.99

	Speed [knots]	Froude number [-]	X_0 = S60_S971, [%]
0	1.44	0.15	6.64
1	1.93	0.20	-3.65
2	2.41	0.25	-5.65
3	2.89	0.30	-1.65
4	3.37	0.35	1.26
5	3.85	0.40	1.53
6	4.33	0.45	-3.73
7	4.81	0.50	-1.22
8	5.30	0.55	1.51

	Speed [knots]	Froude number [-]	X_0 = S60_S971, [N]
0	1.44	0.15	0.16
1	1.93	0.20	-0.17
2	2.41	0.25	-0.42
3	2.89	0.30	-0.22
4	3.37	0.35	0.23
5	3.85	0.40	0.76
6	4.33	0.45	-3.42
7	4.81	0.50	-1.33
8	5.30	0.55	1.74

Figure 6: S60_S971 evolution, difference in [%] and [N] of drag resistance

v. S60_S1174

	Speed [knots]	Froude number [-]	● Total resistance [N], S60_S1174	■ Total resistance [N], S60_S1174_EFD
0	1.44	0.15	2.55	2.45
1	1.93	0.20	4.46	4.42
2	2.41	0.25	7.02	7.08
3	2.89	0.30	12.46	12.60
4	3.37	0.35	20.12	19.68
5	3.85	0.40	49.55	48.30
6	4.33	0.45	80.34	83.24
7	4.81	0.50	100.53	102.30
8	5.30	0.55	112.94	111.86

	Speed [knots]	Froude number [-]	X_0 = S60_S1174, [%]
0	1.44	0.15	4.08
1	1.93	0.20	0.90
2	2.41	0.25	-0.85
3	2.89	0.30	-1.11
4	3.37	0.35	2.24
5	3.85	0.40	2.59
6	4.33	0.45	-3.48
7	4.81	0.50	-1.73
8	5.30	0.55	0.97

	Speed [knots]	Froude number [-]	X_0 = S60_S1174, [N]
0	1.44	0.15	0.10
1	1.93	0.20	0.04
2	2.41	0.25	-0.06
3	2.89	0.30	-0.14
4	3.37	0.35	0.44
5	3.85	0.40	1.25
6	4.33	0.45	-2.90
7	4.81	0.50	-1.77
8	5.30	0.55	1.08

Figure 7: S60_S1174 evolution, difference in [%] and [N] of drag resistance

b. Heave

The dynamic heave response of the Series 60 monohull and catamaran at the different float spacings across different advance speeds are illustrates in the top graph and table of:

- Figure 8: S60_Mono evolution, difference in [%] and [m] of dynamic heave attitude
- Figure 9: S60_S565 evolution, difference in [%] and [m] of dynamic heave attitude
- Figure 10: S60_S768 evolution, difference in [%] and [m] of dynamic heave attitude
- Figure 11: S60_S971 evolution, difference in [%] and [m] of dynamic heave attitude
- Figure 12: S60_S1174 evolution, difference in [%] and [m] of dynamic heave attitude

The middle table displays the relative difference between CFD and EFD as a percentage, while the bottom table shows the absolute differences between CFD and EFD in international units:

$$E\%\ CFD = \frac{CFD - EFD}{EFD} * 100$$

To thoroughly assess results, particularly percentage differences, it is important to consider both percentage and absolute values. In comparisons with towing tank tests, target dynamic heave values are very low, so even minor discrepancies can lead to large percentage errors.

The dynamic heave response error ranges from:

- -15.61 to -5.00 percents and from +0.000 to +0.004 meters for the S60_Mono hull.
- -40.62 to -6.74 percents and from +0.001 to +0.004 meters for the S60_S565 hull.
- -19.05 to +6.70 percents and from -0.001 to +0.002 meters for the S60_S768 hull.
- -23.81 to -3.03 percents and from +0.000 to +0.002 meters for the S60_S971 hull.
- -15.87 to +3.29 percents and from -0.001 to +0.000 meters for the S60_S1174 hull.

The dynamic heave error between the EFD and CFD simulations is on the order of millimetres, demonstrating excellent agreement at most speeds, particularly due to the very similar trends observed in the curves.

However, it is worth noting that the numerical results tend to overestimate the heave compared to the experimental data. Additionally, the Centre of Gravity was estimated based on the hull's volumetric data, as the exact value is not available in the paper. This estimation may lead to a slight difference in the calculation of dynamic heave, as this calculation relies on subtracting the height of the centre of gravity.

It is important to understand that the main objective of this validation case is to validate the prediction of the resistance to forward motion. Therefore, the script used is optimized to accurately predict this resistance while minimizing the computational time.

i. S60_Mono

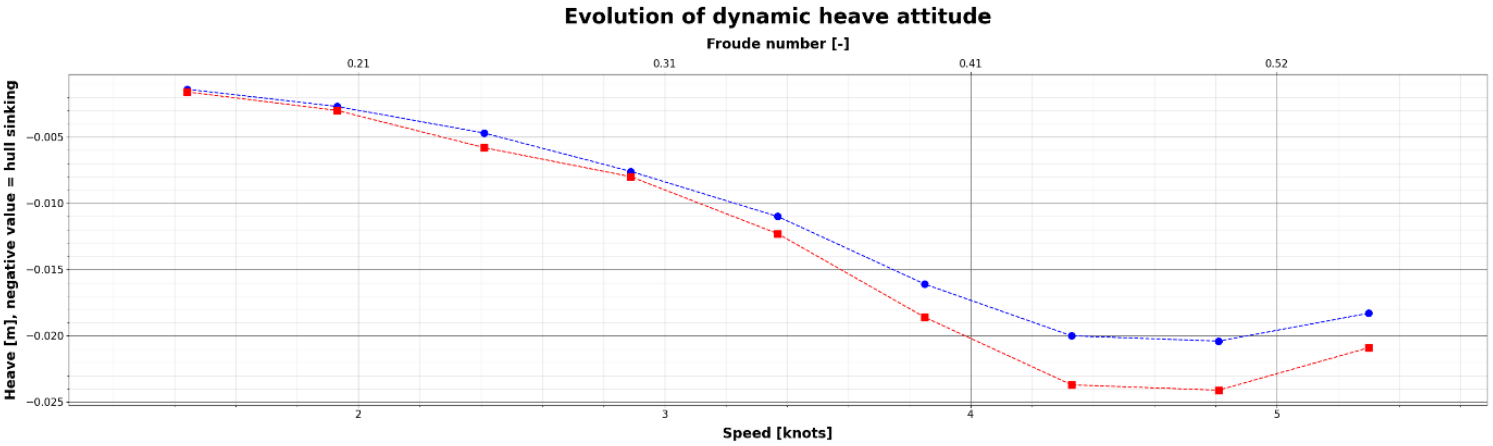

	Speed [knots]	Froude number [-]	● Heave [m], S60_Mono	■ Heave [m], S60_Mono_EFD
0	1.44	0.15	-0.0014	-0.0016
1	1.93	0.20	-0.0027	-0.0030
2	2.41	0.25	-0.0047	-0.0058
3	2.89	0.30	-0.0076	-0.0080
4	3.37	0.35	-0.0110	-0.0123
5	3.85	0.40	-0.0161	-0.0186
6	4.33	0.45	-0.0200	-0.0237
7	4.81	0.50	-0.0204	-0.0241
8	5.30	0.55	-0.0183	-0.0209

	Speed [knots]	Froude number [-]	X_0 = S60_Mono, [%]
0	1.44	0.15	-12.50
1	1.93	0.20	-10.00
2	2.41	0.25	-18.97
3	2.89	0.30	-5.00
4	3.37	0.35	-10.57
5	3.85	0.40	-13.44
6	4.33	0.45	-15.61
7	4.81	0.50	-15.35
8	5.30	0.55	-12.44

	Speed [knots]	Froude number [-]	X_0 = S60_Mono, [m]
0	1.44	0.15	0.000
1	1.93	0.20	0.000
2	2.41	0.25	0.001
3	2.89	0.30	0.000
4	3.37	0.35	0.001
5	3.85	0.40	0.002
6	4.33	0.45	0.004
7	4.81	0.50	0.004
8	5.30	0.55	0.003

Figure 8: S60_Mono evolution, difference in [%] and [m] of dynamic heave attitude

ii. S60_S565

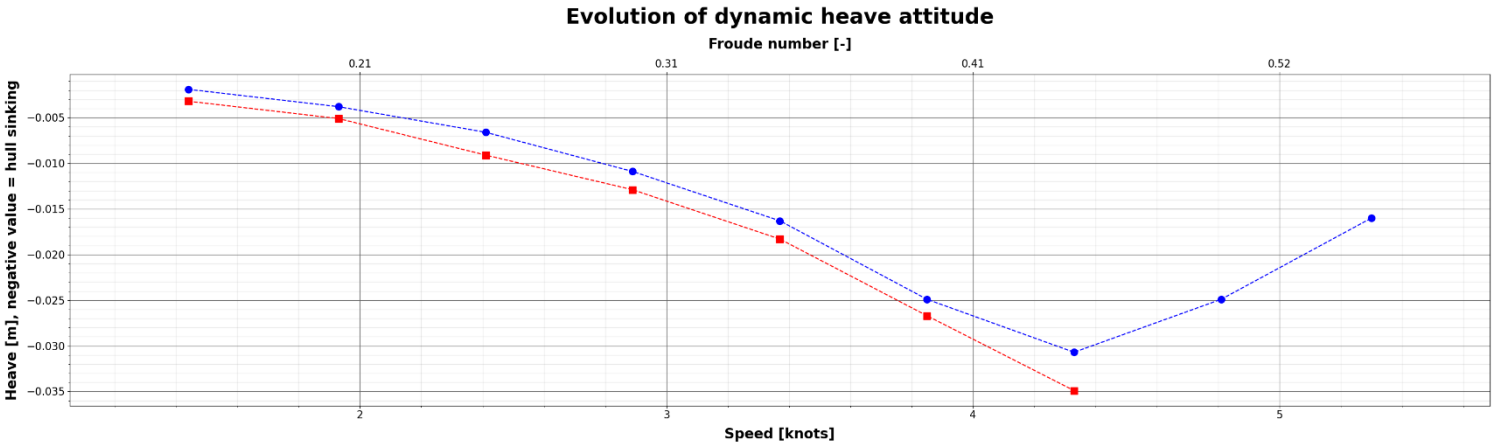

	Speed [knots]	Froude number [-]	● Heave [m], S60_S565	■ Heave [m], S60_S565_EFD
0	1.44	0.15	-0.0019	-0.0032
1	1.93	0.20	-0.0038	-0.0051
2	2.41	0.25	-0.0066	-0.0091
3	2.89	0.30	-0.0109	-0.0129
4	3.37	0.35	-0.0163	-0.0183
5	3.85	0.40	-0.0249	-0.0267
6	4.33	0.45	-0.0307	-0.0349
7	4.81	0.50	-0.0249	X
8	5.30	0.55	-0.0160	X

	Speed [knots]	Froude number [-]	X_0 = S60_S565, [%]
0	1.44	0.15	-40.62
1	1.93	0.20	-25.49
2	2.41	0.25	-27.47
3	2.89	0.30	-15.50
4	3.37	0.35	-10.93
5	3.85	0.40	-6.74
6	4.33	0.45	-12.03

	Speed [knots]	Froude number [-]	X_0 = S60_S565, [m]
0	1.44	0.15	0.001
1	1.93	0.20	0.001
2	2.41	0.25	0.003
3	2.89	0.30	0.002
4	3.37	0.35	0.002
5	3.85	0.40	0.002
6	4.33	0.45	0.004

Figure 9: S60_S565 evolution, difference in [%] and [m] of dynamic heave attitude

iii. S60_S768

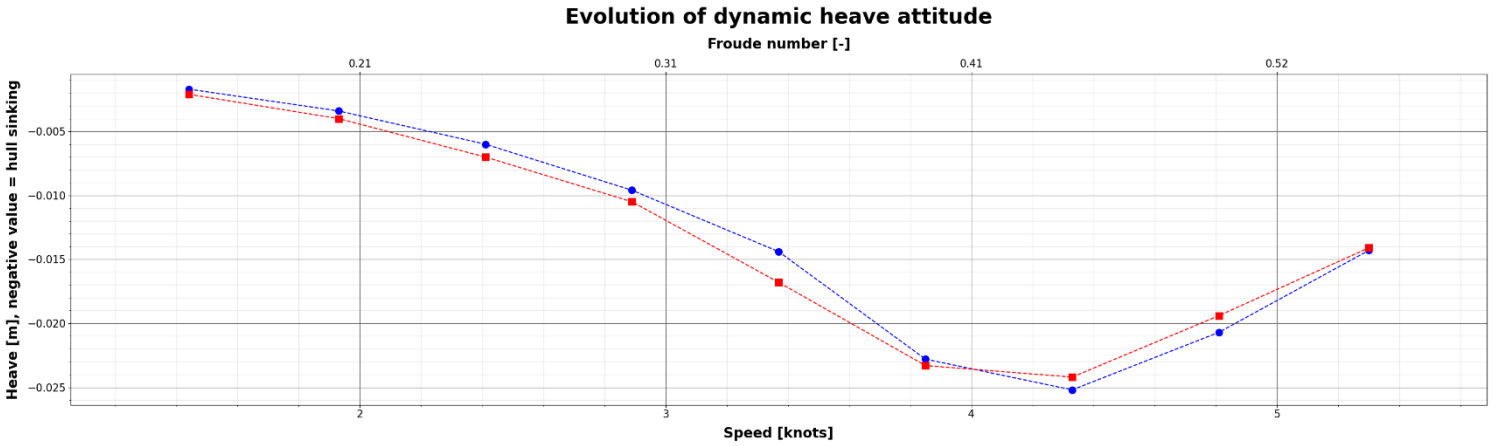

	Speed [knots]	Froude number [-]	● Heave [m], S60_S768	■ Heave [m], S60_S768_EFD
0	1.44	0.15	-0.0017	-0.0021
1	1.93	0.20	-0.0034	-0.0040
2	2.41	0.25	-0.0060	-0.0070
3	2.89	0.30	-0.0096	-0.0105
4	3.37	0.35	-0.0144	-0.0168
5	3.85	0.40	-0.0228	-0.0233
6	4.33	0.45	-0.0252	-0.0242
7	4.81	0.50	-0.0207	-0.0194
8	5.30	0.55	-0.0143	-0.0141

	Speed [knots]	Froude number [-]	X_0 = S60_S768, [%]
0	1.44	0.15	-19.05
1	1.93	0.20	-15.00
2	2.41	0.25	-14.29
3	2.89	0.30	-8.57
4	3.37	0.35	-14.29
5	3.85	0.40	-2.15
6	4.33	0.45	4.13
7	4.81	0.50	6.70
8	5.30	0.55	1.42

	Speed [knots]	Froude number [-]	X_0 = S60_S768, [m]
0	1.44	0.15	0.000
1	1.93	0.20	0.001
2	2.41	0.25	0.001
3	2.89	0.30	0.001
4	3.37	0.35	0.002
5	3.85	0.40	0.001
6	4.33	0.45	-0.001
7	4.81	0.50	-0.001
8	5.30	0.55	-0.000

Figure 10: S60_S768 evolution, difference in [%] and [m] of dynamic heave attitude

iv. S60_S971

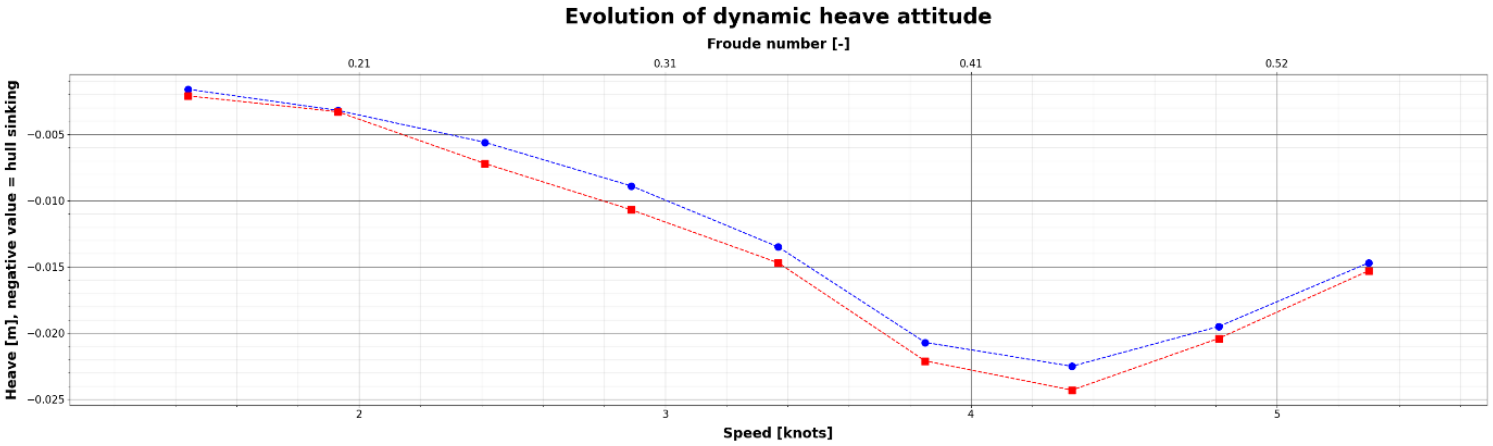

	Speed [knots]	Froude number [-]	● Heave [m], S60_S971	■ Heave [m], S60_S971_EFD
0	1.44	0.15	-0.0016	-0.0021
1	1.93	0.20	-0.0032	-0.0033
2	2.41	0.25	-0.0056	-0.0072
3	2.89	0.30	-0.0089	-0.0107
4	3.37	0.35	-0.0135	-0.0147
5	3.85	0.40	-0.0207	-0.0221
6	4.33	0.45	-0.0225	-0.0243
7	4.81	0.50	-0.0195	-0.0204
8	5.30	0.55	-0.0147	-0.0153

	Speed [knots]	Froude number [-]	X_0 = S60_S971, [%]
0	1.44	0.15	-23.81
1	1.93	0.20	-3.03
2	2.41	0.25	-22.22
3	2.89	0.30	-16.82
4	3.37	0.35	-8.16
5	3.85	0.40	-6.33
6	4.33	0.45	-7.41
7	4.81	0.50	-4.41
8	5.30	0.55	-3.92

	Speed [knots]	Froude number [-]	X_0 = S60_S971, [m]
0	1.44	0.15	0.000
1	1.93	0.20	0.000
2	2.41	0.25	0.002
3	2.89	0.30	0.002
4	3.37	0.35	0.001
5	3.85	0.40	0.001
6	4.33	0.45	0.002
7	4.81	0.50	0.001
8	5.30	0.55	0.001

Figure 11: S60_S971 evolution, difference in [%] and [m] of dynamic heave attitude

v. S60_S1174

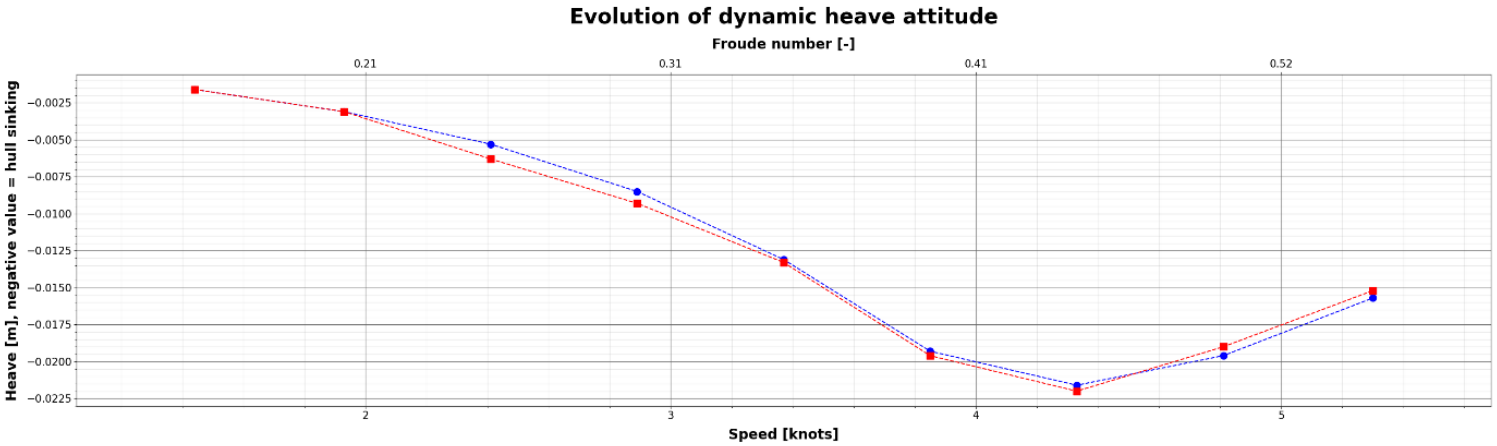

	Speed [knots]	Froude number [-]	● Heave [m], S60_S1174	■ Heave [m], S60_S1174_EFD
0	1.44	0.15	-0.0016	-0.0016
1	1.93	0.20	-0.0031	-0.0031
2	2.41	0.25	-0.0053	-0.0063
3	2.89	0.30	-0.0085	-0.0093
4	3.37	0.35	-0.0131	-0.0133
5	3.85	0.40	-0.0193	-0.0196
6	4.33	0.45	-0.0216	-0.0220
7	4.81	0.50	-0.0196	-0.0190
8	5.30	0.55	-0.0157	-0.0152

	Speed [knots]	Froude number [-]	X_0 = S60_S1174, [%]
0	1.44	0.15	-0.00
1	1.93	0.20	-0.00
2	2.41	0.25	-15.87
3	2.89	0.30	-8.60
4	3.37	0.35	-1.50
5	3.85	0.40	-1.53
6	4.33	0.45	-1.82
7	4.81	0.50	3.16
8	5.30	0.55	3.29

	Speed [knots]	Froude number [-]	X_0 = S60_S1174, [m]
0	1.44	0.15	0.000
1	1.93	0.20	0.000
2	2.41	0.25	0.001
3	2.89	0.30	0.001
4	3.37	0.35	0.000
5	3.85	0.40	0.000
6	4.33	0.45	0.000
7	4.81	0.50	-0.001
8	5.30	0.55	-0.000

Figure 12: S60_S1174 evolution, difference in [%] and [m] of dynamic heave attitude

c. Pitch

The dynamic pitch response of the Series 60 monohull and catamaran at the different float spacings across different advance speeds are illustrates in the top graph and table of:

- Figure 13: S60_Mono evolution, difference in [%] and [deg] of dynamic pitch attitude
- Figure 14: S60_S565 evolution, difference in [%] and [deg] of dynamic pitch attitude
- Figure 15: S60_S768 evolution, difference in [%] and [deg] of dynamic pitch attitude
- Figure 16: S60_S971 evolution, difference in [%] and [deg] of dynamic pitch attitude
- Figure 17: S60_S1174 evolution, difference in [%] and [deg] of dynamic pitch attitude

The middle table displays the relative difference between CFD and EFD as a percentage, while the bottom table shows the absolute differences between CFD and EFD in international units:

$$E\%\ CFD = \frac{CFD - EFD}{EFD} * 100$$

To thoroughly assess results, particularly percentage differences, it is important to consider both percentage and absolute values. In comparisons with towing tank tests, target dynamic pitch values are very low, so even minor discrepancies can lead to large percentage errors.

The dynamic pitch response error ranges from

- -74.88 to +76.52 percents and from +0.022 to +0.531 degrees for the S60_Mono hull.
- -72.34 to +331.09 percents and from +0.030 to +0.937 degrees for the S60_S565 hull.
- -62.57 to +46.05 percents and from +0.022 to +0.629 degrees for the S60_S768 hull.
- -65.25 to +59.36 percents and from +0.040 to +0.823 degrees for the S60_S971 hull.
- -89.24 to +44.06 percents and from +0.031 to +0.718 degrees for the S60_S1174 hull.

In the case of the dynamic pitch response, larger discrepancies exist between CFD and EFD.

However, the trend of the curves is followed for all configurations.

It is worth noting that the numerical results tend to overestimate the heave compared to the experimental data. Moreover, the gap between CFD and EFD increases with the rise in speed.

It is important to understand that the main objective of this validation case is to validate the prediction of the resistance to forward motion. Therefore, the script used is optimized to accurately predict this resistance while minimizing the computational time.

i. S60_Mono

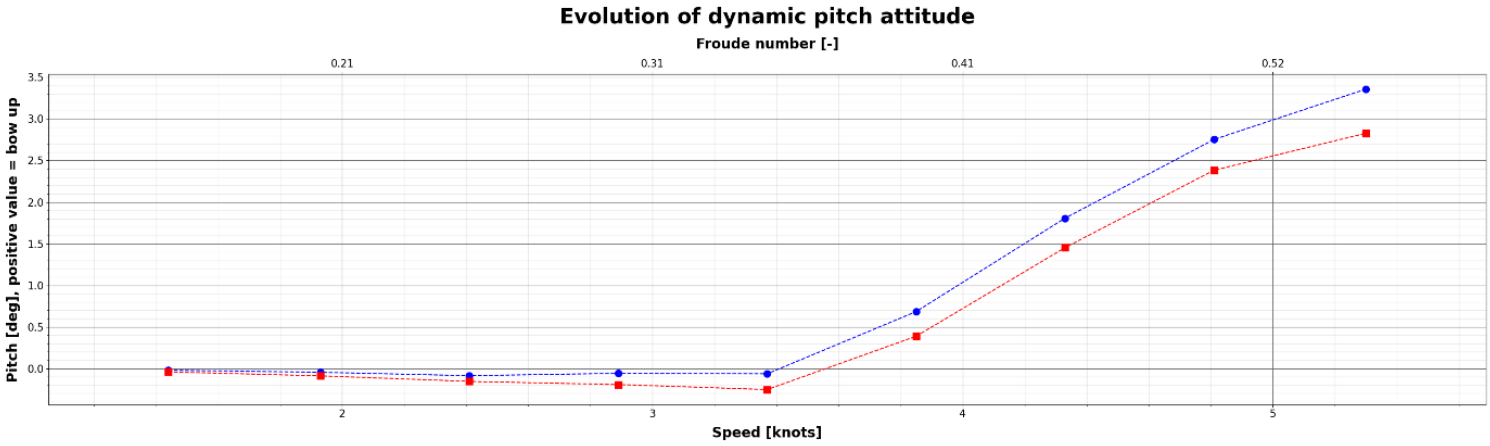

	Speed [knots]	Froude number [-]	● Pitch [deg], S60_Mono	■ Pitch [deg], S60_Mono_EFD
0	1.44	0.15	-0.0198	-0.0415
1	1.93	0.20	-0.0460	-0.0882
2	2.41	0.25	-0.0864	-0.1553
3	2.89	0.30	-0.0582	-0.1931
4	3.37	0.35	-0.0636	-0.2532
5	3.85	0.40	0.6842	0.3876
6	4.33	0.45	1.8073	1.4533
7	4.81	0.50	2.7532	2.3836
8	5.30	0.55	3.3592	2.8284

	Speed [knots]	Froude number [-]	X_0 = S60_Mono, [%]
0	1.44	0.15	-52.29
1	1.93	0.20	-47.85
2	2.41	0.25	-44.37
3	2.89	0.30	-69.86
4	3.37	0.35	-74.88
5	3.85	0.40	76.52
6	4.33	0.45	24.36
7	4.81	0.50	15.51
8	5.30	0.55	18.77

	Speed [knots]	Froude number [-]	X_0 = S60_Mono, [deg]
0	1.44	0.15	0.022
1	1.93	0.20	0.042
2	2.41	0.25	0.069
3	2.89	0.30	0.135
4	3.37	0.35	0.190
5	3.85	0.40	0.297
6	4.33	0.45	0.354
7	4.81	0.50	0.370
8	5.30	0.55	0.531

Figure 13: S60_Mono evolution, difference in [%] and [deg] of dynamic pitch attitude

ii. S60_S565

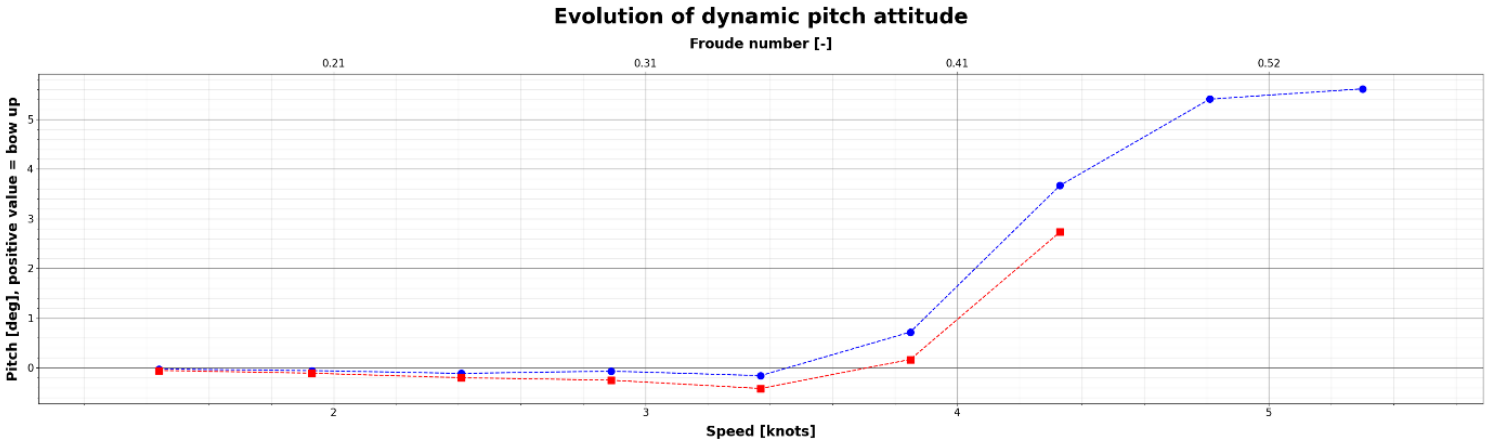

	Speed [knots]	Froude number [-]	● Pitch [deg], S60_S565	■ Pitch [deg], S60_S565_EFD
0	1.44	0.15	-0.0245	-0.0549
1	1.93	0.20	-0.0582	-0.1100
2	2.41	0.25	-0.1143	-0.2014
3	2.89	0.30	-0.0694	-0.2509
4	3.37	0.35	-0.1591	-0.4179
5	3.85	0.40	0.7182	0.1666
6	4.33	0.45	3.6690	2.7325
7	4.81	0.50	5.4074	X
8	5.30	0.55	5.6144	X

	Speed [knots]	Froude number [-]	X_0 = S60_S565, [%]
0	1.44	0.15	-55.37
1	1.93	0.20	-47.09
2	2.41	0.25	-43.25
3	2.89	0.30	-72.34
4	3.37	0.35	-61.93
5	3.85	0.40	331.09
6	4.33	0.45	34.27

	Speed [knots]	Froude number [-]	X_0 = S60_S565, [deg]
0	1.44	0.15	0.030
1	1.93	0.20	0.052
2	2.41	0.25	0.087
3	2.89	0.30	0.181
4	3.37	0.35	0.259
5	3.85	0.40	0.552
6	4.33	0.45	0.937

Figure 14: S60_S565 evolution, difference in [%] and [deg] of dynamic pitch attitude

iii. S60_S768

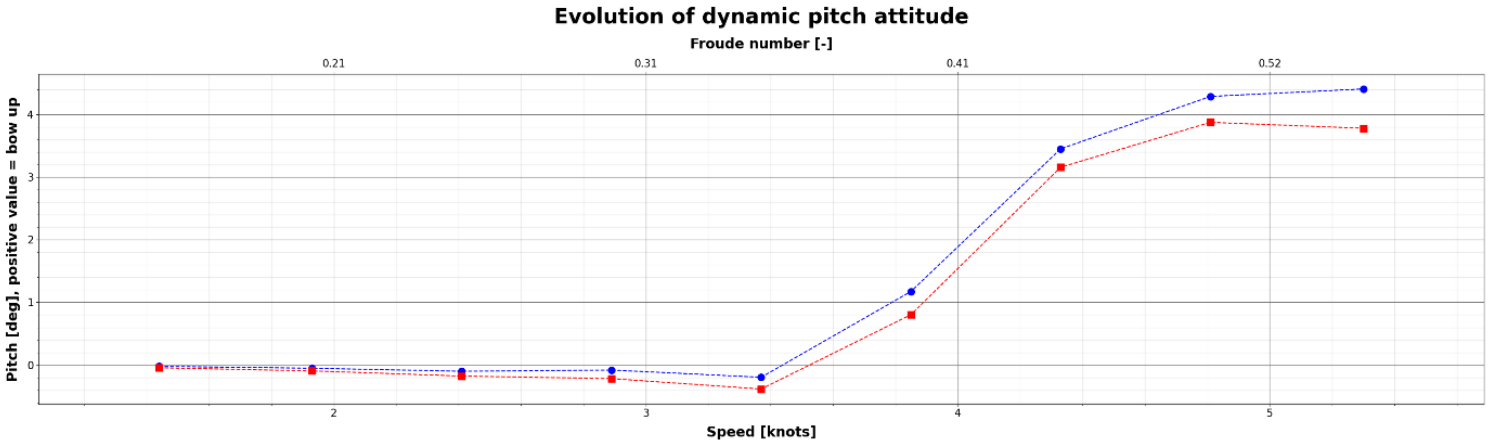

	Speed [knots]	Froude number [-]	● Pitch [deg], S60_S768	■ Pitch [deg], S60_S768_EFD
0	1.44	0.15	-0.0223	-0.0444
1	1.93	0.20	-0.0522	-0.0951
2	2.41	0.25	-0.1003	-0.1770
3	2.89	0.30	-0.0817	-0.2183
4	3.37	0.35	-0.1965	-0.3843
5	3.85	0.40	1.1744	0.8041
6	4.33	0.45	3.4534	3.1597
7	4.81	0.50	4.2911	3.8776
8	5.30	0.55	4.4104	3.7813

	Speed [knots]	Froude number [-]	X_0 = S60_S768, [%]
0	1.44	0.15	-49.77
1	1.93	0.20	-45.11
2	2.41	0.25	-43.33
3	2.89	0.30	-62.57
4	3.37	0.35	-48.87
5	3.85	0.40	46.05
6	4.33	0.45	9.30
7	4.81	0.50	10.66
8	5.30	0.55	16.64

	Speed [knots]	Froude number [-]	X_0 = S60_S768, [deg]
0	1.44	0.15	0.022
1	1.93	0.20	0.043
2	2.41	0.25	0.077
3	2.89	0.30	0.137
4	3.37	0.35	0.188
5	3.85	0.40	0.370
6	4.33	0.45	0.294
7	4.81	0.50	0.413
8	5.30	0.55	0.629

Figure 15: S60_S768 evolution, difference in [%] and [deg] of dynamic pitch attitude

iv. S60_S971

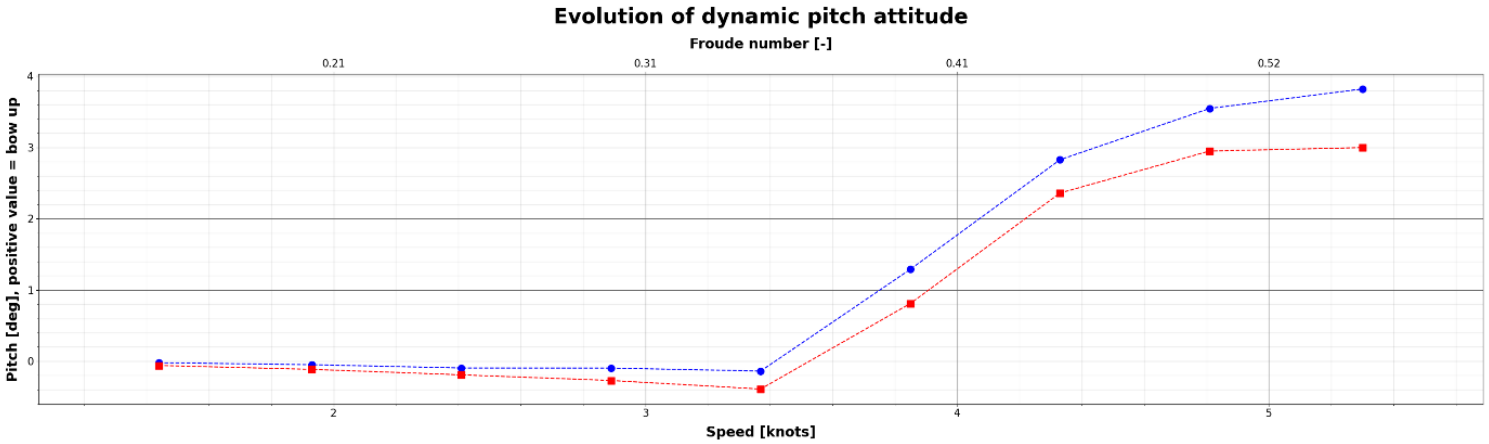

	Speed [knots]	Froude number [-]	● Pitch [deg], S60_S971	■ Pitch [deg], S60_S971_EFD
0	1.44	0.15	-0.0212	-0.0610
1	1.93	0.20	-0.0496	-0.1149
2	2.41	0.25	-0.0960	-0.1923
3	2.89	0.30	-0.0968	-0.2711
4	3.37	0.35	-0.1386	-0.3910
5	3.85	0.40	1.2900	0.8095
6	4.33	0.45	2.8281	2.3604
7	4.81	0.50	3.5482	2.9503
8	5.30	0.55	3.8217	2.9988

	Speed [knots]	Froude number [-]	X_0 = S60_S971, [%]
0	1.44	0.15	-65.25
1	1.93	0.20	-56.83
2	2.41	0.25	-50.08
3	2.89	0.30	-64.29
4	3.37	0.35	-64.55
5	3.85	0.40	59.36
6	4.33	0.45	19.81
7	4.81	0.50	20.27
8	5.30	0.55	27.44

	Speed [knots]	Froude number [-]	X_0 = S60_S971, [deg]
0	1.44	0.15	0.040
1	1.93	0.20	0.065
2	2.41	0.25	0.096
3	2.89	0.30	0.174
4	3.37	0.35	0.252
5	3.85	0.40	0.481
6	4.33	0.45	0.468
7	4.81	0.50	0.598
8	5.30	0.55	0.823

Figure 16: S60_S971 evolution, difference in [%] and [deg] of dynamic pitch attitude

v. S60_S1174

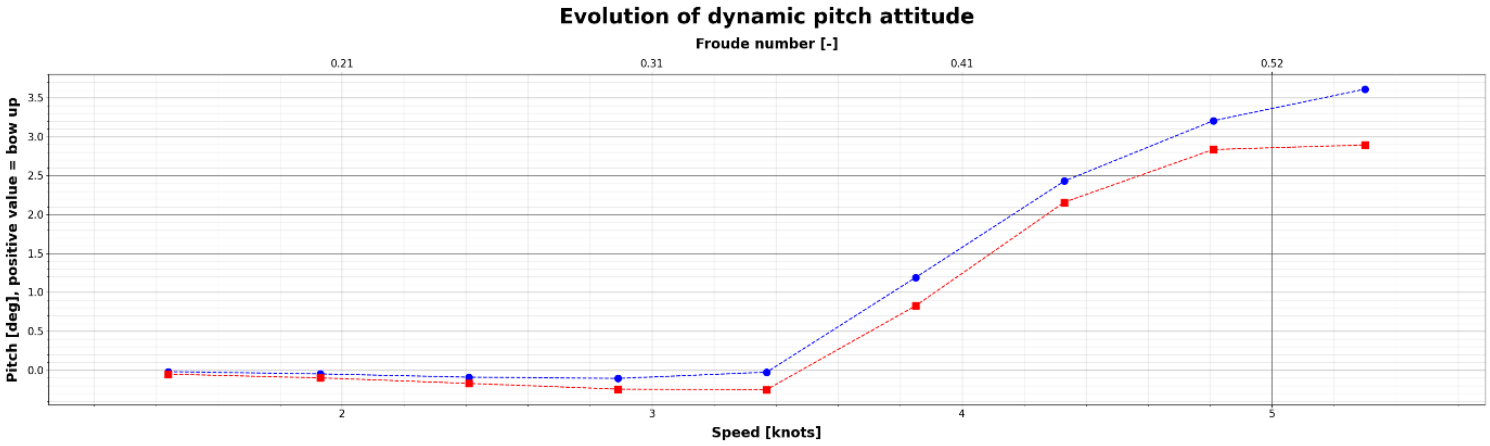

	Speed [knots]	Froude number [-]	● Pitch [deg], S60_S1174	■ Pitch [deg], S60_S1174_EFD
0	1.44	0.15	-0.0206	-0.0517
1	1.93	0.20	-0.0492	-0.1002
2	2.41	0.25	-0.0908	-0.1713
3	2.89	0.30	-0.1067	-0.2451
4	3.37	0.35	-0.0270	-0.2509
5	3.85	0.40	1.1892	0.8255
6	4.33	0.45	2.4297	2.1577
7	4.81	0.50	3.2049	2.8350
8	5.30	0.55	3.6118	2.8935

	Speed [knots]	Froude number [-]	X_0 = S60_S1174, [%]
0	1.44	0.15	-60.15
1	1.93	0.20	-50.90
2	2.41	0.25	-46.99
3	2.89	0.30	-56.47
4	3.37	0.35	-89.24
5	3.85	0.40	44.06
6	4.33	0.45	12.61
7	4.81	0.50	13.05
8	5.30	0.55	24.82

	Speed [knots]	Froude number [-]	X_0 = S60_S1174, [deg]
0	1.44	0.15	0.031
1	1.93	0.20	0.051
2	2.41	0.25	0.081
3	2.89	0.30	0.138
4	3.37	0.35	0.224
5	3.85	0.40	0.364
6	4.33	0.45	0.272
7	4.81	0.50	0.370
8	5.30	0.55	0.718

Figure 17: S60_S1174 evolution, difference in [%] and [deg] of dynamic pitch attitude

5. Free surface elevations

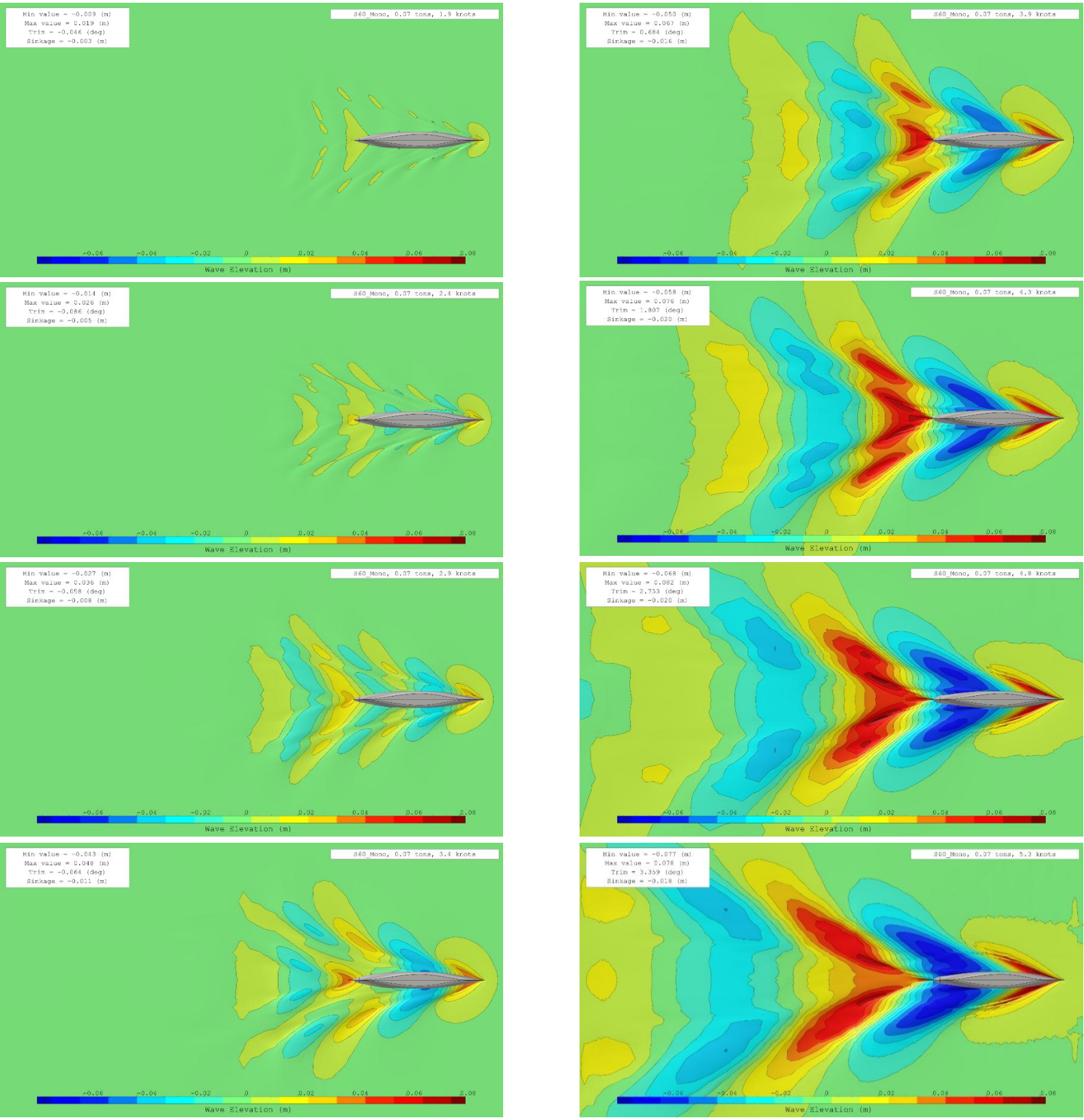

Figure 18: Free surface evolution of S60_Mono (same scale) from 1.9 to 5.3 knots

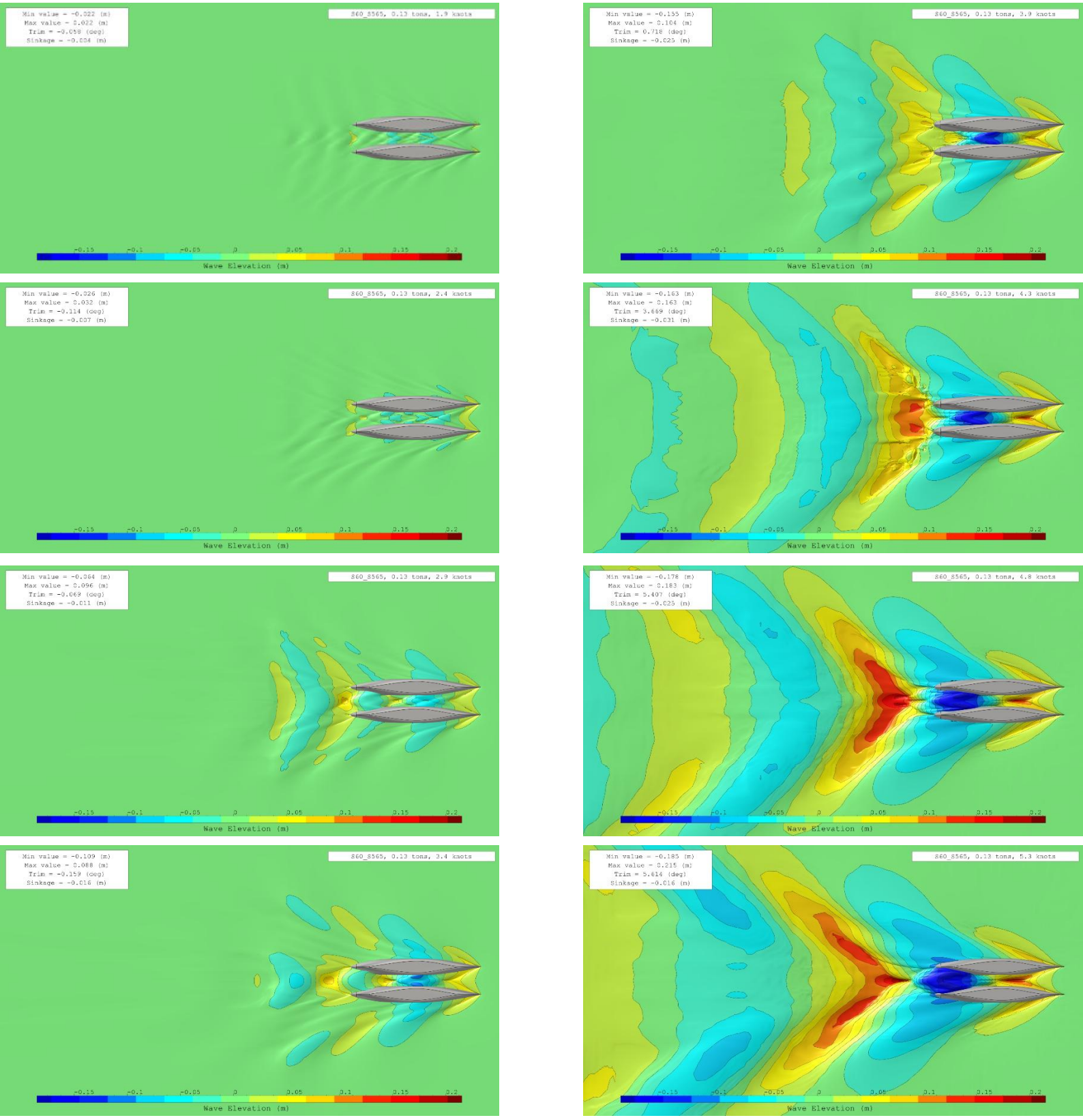

Figure 19: Free surface evolution of S60_S565 (same scale) from 1.9 to 5.3 knots

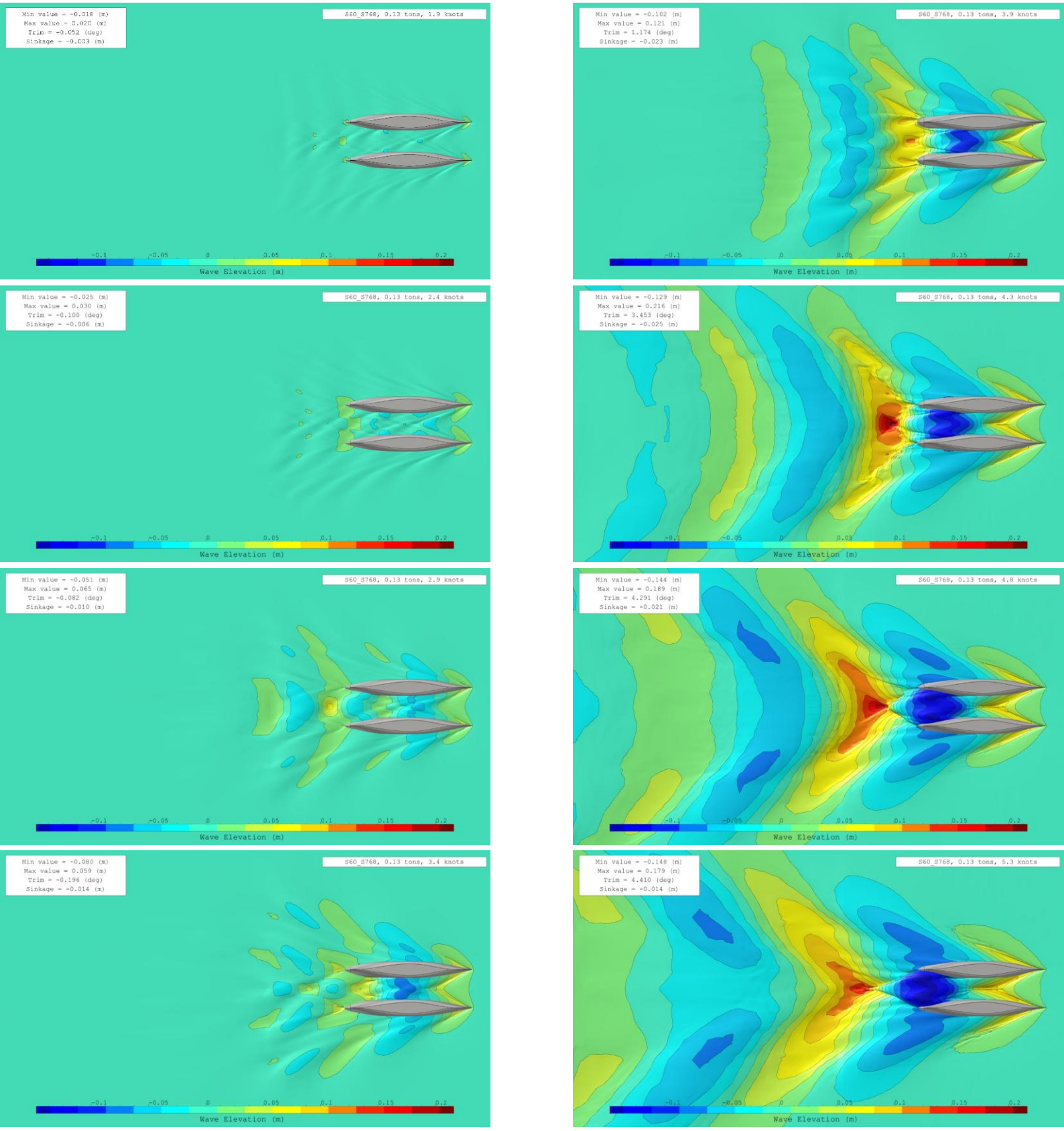

Figure 20: Free surface evolution of S60_S768 (same scale) from 1.9 to 5.3 knots

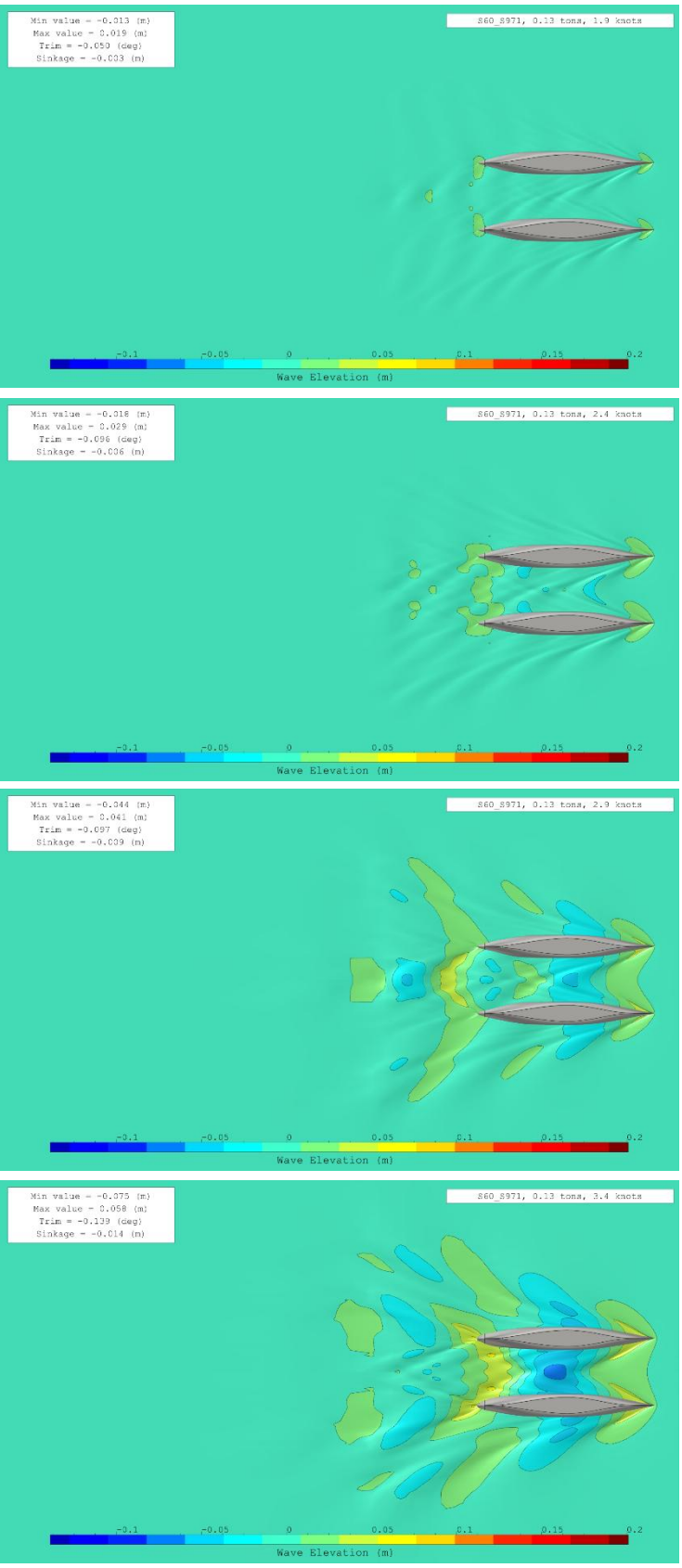

Figure 21: Free surface evolution of S60_S971 (same scale) from 1.9 to 5.3 knots

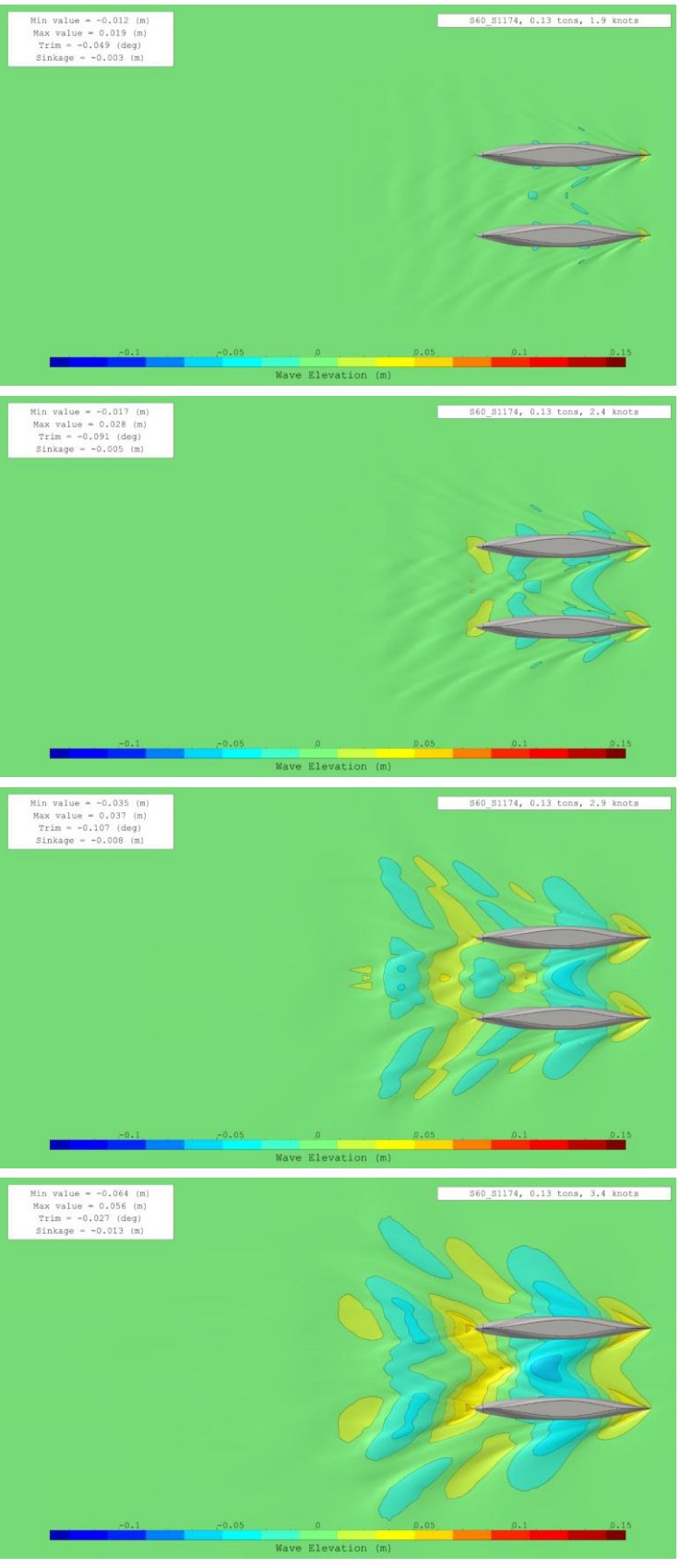

Figure 22: Free surface evolution of S60_S1174 (same scale) from 1.9 to 5.3 knots

6. Computational time comparison

Figure 23 compares the simulation times for a medium mesh configuration across the monohull case and catamaran cases with different float spacings.

As expected, computation time increases for Froude numbers above 0.4, due to the larger wake and more pronounced wave-induced motions. Additionally, in the catamaran cases, the interaction wave becomes more significant, leading to stronger hydrodynamic interference between the floats. This effect forces the Adaptive Grid Refinement to refine the mesh between the floats, where noticeable pressure gradient variations occur, further increasing computational cost.

For the monohull case, S60_Mono, the total simulation time for nine speeds is 23.59 hours, averaging 2.62 hours per speed. In comparison, the catamaran configurations exhibit higher computational costs due to increased wave interactions and the fact that a catamaran is essentially the sum of two monohulls, leading to a larger computational domain and more complex flow interactions:

- S60_S565: 43.72 hours total, averaging 4.86 hours per speed
- S60_S768: 40.40 hours total, averaging 4.49 hours per speed
- S60_S971: 40.79 hours total, averaging 4.53 hours per speed
- S60_S1174: 44.41 hours total, averaging 4.93 hours per speed

These results highlight the computational impact of float spacing, with narrower configurations requiring more refinement and leading to longer simulation times.

Given the highly precise results compared to the experimental data, this simulation time is exceptionally efficient.

	Speed [knots]	Froude number [-]	● Core [-]	S60_Mono	● Core [-]	S60_S565	● Core [-]	S60_S768	● Core [-]	S60_S971	● Core [-]	S60_S1174
0	1.44	0.15	18	0.82	32	1.35	32	1.30	32	1.43	32	1.43
1	1.93	0.20	18	0.82	32	1.60	32	1.50	32	1.53	32	1.67
2	2.41	0.25	18	1.27	32	2.08	32	2.13	32	2.20	32	2.70
3	2.89	0.30	20	3.20	32	4.42	32	2.43	32	3.45	32	4.30
4	3.37	0.35	20	3.35	32	4.25	32	4.13	32	4.08	32	6.02
5	3.85	0.40	20	1.50	32	6.67	32	6.18	32	6.37	32	6.27
6	4.33	0.45	20	4.13	32	8.35	32	7.78	32	7.03	32	7.40
7	4.81	0.50	20	4.18	32	7.93	32	7.53	32	7.18	32	7.17
8	5.30	0.55	20	4.32	32	7.07	32	7.42	32	7.52	32	7.45

Figure 23: Computational time in hours

7. Conclusion

This report presents a validation study, conducted to predict the calm-water hydrodynamic resistance of the Series 60 in monohull and catamaran configuration across varying float spacings and advance speeds, comparing results obtained using NepTech's digital towing tank with available experimental data from the paper " *Experimental Assessment of Interference Resistance for a Series 60 Catamaran in Free and Fixed Trim-Sinkage Conditions* ".

The findings highlight a strong correlation between the numerical and experimental results, largely due to the highly similar trends observed in the curves:

- For drag resistance, errors range from -5.25% to +7.88% across different hull configurations, with differences on the order of Newtons.
- The dynamic heave response also showed promising results, with errors on the order of millimetres, although numerical simulations tend to slightly overestimate dynamic heave values.
- Larger discrepancies were observed in the dynamic pitch response, with the numerical model tending to overestimate dynamic pitch.

Some discrepancies observed between CFD and EFD results can also be attributed to uncertainties inherent in the experimental measurements.

Crucially, the primary focus of this validation was to assess the prediction of forward motion resistance, for which NepTech's digital towing tank was specifically optimized to balance computational efficiency with accuracy.

This report confirms NepTech's ability to accurately and efficiently predict the dynamic behaviour of a catamaran vessel transitioning from low to medium speeds across varying float spacings. By utilizing NepTech’s fully automated digital towing tank equipped with the latest advanced modelling tools, we conclude that simulations of similar flow types will yield reliable results.

Bibliography

Souto-Iglesias, A., Fernandez-Gutierrez, D., & Perez-Rojas, L. (2012). Experimental assessment of interference resistance for a Series 60 catamaran in free and fixed trim-sinkage conditions. *Ocean Engineering*. Récupéré sur https://doi.org/10.1016/j.oceaneng.2012.06.008